IEEE Access
Multidisciplinary | Rapid Review | Open Access Journal

Received April 2, 2020, accepted April 18, 2020, date of publication April 22, 2020, date of current version May 7, 2020.

Digital Object Identifier 10.1109/ACCESS.2020.2989508

Risk Assessment of Offshore Micro Integrated Energy System Based on Fluid Mosaic Model

ANAN ZHANG, (Senior Member, IEEE), GAOQIANG PENG, WEI YANG, (Member, IEEE), GUANGLONG QU, (Member, IEEE), AND HUANG HUANG

School of Electrical and Information Engineering, Southwest Petroleum University, Chengdu 610500, China

Corresponding author: Anan Zhang (ananzhang@hotmail.com)

This work was supported in part by the National Key Research and Development Program of China under Grant 2017YFE0112600.

ABSTRACT Offshore micro integrated energy systems are the basis of offshore oil and gas engineering. In order to evaluate its operational risks and ensure the safe development of marine resources, a risk assessment scheme for offshore micro integrated energy systems based on a risk fluid mosaic model is proposed. Aiming at the current situation that the traditional equipment material-energy conversion model has a large amount of modeling and does not fully reflect the system structure, a material-energy conversion model based on unified modeling is constructed, and a risk function is introduced to analyze the material-energy of the power equipment under risk conversion; At the same time, a risk fluid mosaic model based on the system structure and material-energy carrier is constructed to describe the dynamic behavior of risk from the material-energy flow; Aiming at the fact that the traditional risk grading model cannot reflect the overall risk of the system when multiple risks are involved, a multi-weighted system risk grading model is proposed to describe the overall risk situation of the system under multiple risks. The validity and rationality of the model and method proposed in this paper is verified by using an offshore oil and gas platform in the Bohai Sea as a simulation example.

INDEX TERMS Offshore micro integrated energy system, unified modeling, risk fluid mosaic model, risk grading, risk assessment.

I. INTRODUCTION

Offshore oil and gas engineering is of great significance to achieve sustainable energy development [1]. Offshore micro integrated energy system (OMIES) is an important way for offshore oil and gas development [2], [3]. It not only couples multiple energy and material flows, but also faces various risks due to the complex marine environmental factors. In order to ensure the safe and stable operation of OMIES, it is necessary to scientifically control its risks.

The reference [4] summarizes the current research status of the reliability of component modeling, system robust analysis, and coupled risk analysis in the energy internet. Reference [5] summarized the research status and prospects of integrated energy system reliability and risk modeling, evaluation algorithms and indicators. Reference [6], [7] established the material-energy conversion model of the main equipment by describing the structure of the energy system, However, the modeling work is complicated, and there is no sufficient description of system structure. Reference [8] proposed a risk assessment method based on the steady-state power flow of the coupled system and the optimal load reduction model, which took into account the random risks of new energy output and load fluctuations, but the analysis of random risk-induced factors of system output equipment was not complete. Reference [9] aimed at assessing the reliability of the electro-thermal interconnection system, and established an evaluation scheme based on the client's maximum thermal power output model and a reliability index based on electro-thermal characteristics. Reference [10] constructed an electro-thermal coupled power flow algorithm based on the steam medium, and proposed a risk assessment scheme based on supply-demand benefits. Although the above research has proposed risk and reliability assessment schemes from different perspectives, it is not clear enough about the coupling. Reference [11] modeled the Energy-Hub energy distribution process and analyzed the impact of gas network faults on the power grid. Reference [12] transferred the uncertainty of the gas network to the failure of the gas turbine and described the characteristics of risk transmission through coupled equipment. Reference [13] established a reliability model of complex behaviors among different subsystems of

The associate editor coordinating the review of this manuscript and approving it for publication was Zhouyang Ren.

the energy system, and analyzed the influence of control methods on system reliability. Reference [14] analyzed the electric-gas coupling system in detail, and studied the impact of natural gas unit failure on the power system cascading failure. Reference [15] proposed a general risk assessment model for combined power and natural gas networks, which quantitatively analyzed the system risks considering power and natural gas network failures. Reference [16] established a system reliability model based on intelligent agent communication and energy hubs, and realized reliability evaluation with fault location, isolation and recovery functions. Reference [17] based on the impact of energy storage on energy supply, established a reliability model under different operating strategies of the energy storage link of the integrated energy system, and quantitatively analyzed the relationship between multiple energy storage and energy supply reliability. Although the above-mentioned risk and reliability analysis based on coupled power flow and Energy-Hub model can reflect the change of risk with energy flow, it ignores the material-risk transfer relationship in the system. Reference [18], [19] established a risk grading system model for power systems, but it's difficult to characterize the overall system risk when multiple risks are involved.

This article introduces a risk function that includes the risk factors of equipment, builds a material-energy conversion model of the output device based on the risk function, characterizes the material-energy conversion relationship under risk, and establishes a risk fluid mosaic model based on the system structure, which analyzes the dynamic behavior of risk through energy-material flow. In addition, a multi-weight system risk grading model is constructed in this model, which can scientifically evaluate the operating risk of OMIES.

II. THE RISK MODEL OF OMIES

A. THE REAL-TIME OUTAGE PROBABILITY MODEL OF EQUIPMENTS

As shown in Figure 1, OMIES usually consists of living, energy supply and production process systems, which are a variety of energy and material flow coupled systems. Unlike conventional integrated energy systems, the energy between OMIES is more closely linked, and energy regulation and scheduling are difficult to rely on external systems. Besides, the importance of OMIES requires it to have more reliable energy transmission and supply than conventional integrated energy systems. OMIES is powered by natural gas or diesel, but fluctuations in material flow will cause uncertainty in energy supply, and fluctuations in energy supply such as electricity and heat will directly affect the stable operation of platform production and process systems.

In OMIES, the equipment operation-stop status is affected by factors such as the offshore operating environment and real-time status. Therefore, three factors are considered into a two-state outage model including: equipment aging,

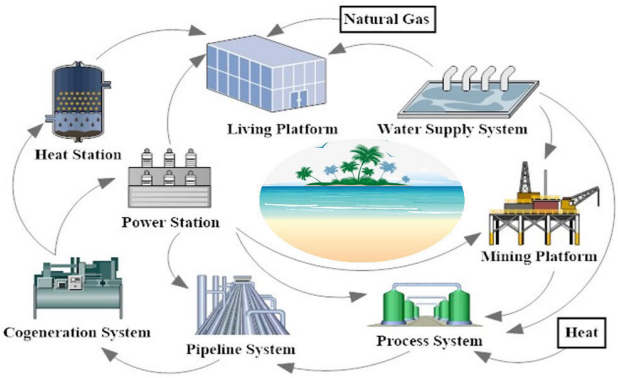

FIGURE 1. Structure diagram of OMIES.

weather, and real-time operation status of the equipment-outage [20]–[23]. The real-time outage probability model is as follows: (1)-(2)

$$\lambda_{\Sigma} = \lambda_{old} + \lambda_{ave}\frac{Z+S}{S}R - \lambda_{ave}\frac{Z+S}{S}(1-R) \tag{1}$$

$$P = \begin{cases} 1 - e^{-\lambda_2 t} & \xi_{\min}^{\text{nor}} \le \xi \le \xi_{\min}^{\text{nor}} \\ & \xi \le \xi_{\min} \text{ or} \\ 1 & \xi \ge \xi_{\max} \\ F\left(\xi, \xi_{\max}^{\text{nor}}, \xi_{\min}^{\text{nor}}, \right. & \\ \quad \left. \xi_{\max}, \xi_{\min}\right)\left(1 - e^{-\lambda_2 t}\right) & \xi_{\min} \le \xi \le \xi_{\max}^{\text{nor}} \text{ or} \\ & \xi_{\max}^{\text{nor}} \le \xi \le \xi_{\max} \end{cases} \tag{2}$$

where λ_{Σ} is the comprehensive equipment outage rate; λ_{old} is the equipment aging failure rate; λ_{ave} is the average equipment failure rate; Z is the time period when the device is in normal weather; S is the time period when the device is in severe weather; R is the failure rate of the device under severe weather; P is the time outage probability of the device in real-time; $F(\xi, \xi_{max}^{nor}, \xi_{min}^{nor}, \xi_{max}, \xi_{min})$ is the effect function of the equipment real-time operating parameters on the equipment outage probability; ξ is the relevant parameters of the equipment operation; ξ_{max}^{nor} is the maximum parameter value for the normal operation of the device; ξ_{min}^{nor} is the minimum parameter value for the normal operation of the device; ξ_{max} is the maximum parameter value of the equipment between the critical conditions of operation and shutdown; ξ_{min} is the minimum parameter value of the equipment between the critical conditions of operation and shutdown.

B. THE MATERIAL-ENERGY RISK CONVERSION MODEL BASED ON UNIFIED MODELING

Figure 2 is the OMIES material-energy flow diagram, which reflects the process of material and energy conversion in the system through various types of equipment.

Traditional material-energy conversion takes equipment as the basic unit. After detailed analysis of the system structure, the material-energy input-output relationship is modeled

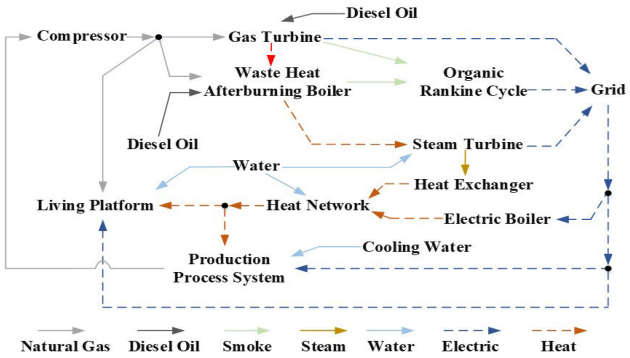

FIGURE 2. Material-energy flow diagram of OMIES.

according to the structure of different equipment [6], [7]. However, for systems with many types of output equipment, this modeling method will make the modeling scale large and fail to reflect the correlation between the output equipment. This section uses a unified modeling method to describe the material-energy conversion relationship of OMIES output equipment. In the unified modeling process, the material-energy source of the system is constant. It is converted into different forms of materials and energy through various types of equipment. Taking OMIES as an example, the system has material-energy conversion mode such as electricity to heat, gas to heat, and gas to electricity, but all the energy of the system comes from associated gas and diesel through different forms of conversion, so the unified modeling method is used to uniformly process the material-energy sources of all output equipment. The function *F(x1, x2, x3 . . .)* is used to describe the system structure that affects the output of the device, and the system material-energy conversion relationship is expressed in a unified model. In addition, the traditional material-energy conversion model cannot reflect the output status of the equipment under risk, and the material-energy relationship of the equipment under the risk can reflect the change in the amount of equipment material-energy conversion when the risk occurs. Therefore, a risk function is introduced into the material energy conversion model based on the unified modeling method, and a risk output model of the device is constructed, and the material energy conversion relationship under risk is described. The material-energy risk conversion model based on unified modeling is shown in equations (3)-(6).

$$E_m = \sum_{i=1}^{a} q_i V_i F(x_1, x_2, x_3 \ldots) f(\alpha) \quad (3)$$

$$Q_n = \sum_{j=1}^{b} q_j V_j F(x_1, x_2, x_3 \ldots) f(\alpha) \quad (4)$$

$$f(\alpha) = \frac{\prod_{k1=1}^{M} \alpha_{k1} \cdot (\sum_{k2=1}^{N} \alpha_{k2})}{N} \quad (5)$$

$$F(x_1, x_2, x_3 \ldots) = \prod_{K1=1}^{n} x_{K1} \cdot (\sum_{K2=1}^{m} x_{K2}) \quad (6)$$

where E_m is the power output of a device; Q_n is the thermal output of a device; V_i is the i-th fuel input of the power output device; q_i is the i-th calorific value of the fuel; V_j is the j-th fuel input of the heat output device; q_j is the calorific value of the j-th fuel; $F(x_1,x_2,x_3\ldots)$ is the mathematical relationship between fuel feed and energy output, $x_1, x_2, x_3 \ldots$ are factors that affect the amount of feed and energy output, Which includes the factors affecting the structure of the device and the system. The value is $0 \sim 1$, x_{K1}, x_{K2} represents the system cascade and parallel parts. The expression of $F(x_1,x_2,x_3\ldots)$ is determined by the device and the system structure and can be expressed as a substance-energy conversion factor represented by a constant. $f(\alpha)$ is the risk function, α is the risk impact factor, and the value is $0 \sim 1$. The expression of $f(\alpha)$ is determined by the external risk, equipment risk and system structure, and M and N are constants related to the system structure.

Compared with the traditional modeling method, the unified modeling method reduces the system modeling workload in the material-energy conversion model in OMIES, unifies the input and output of material-energy, and improves the problem of insufficient system structure correlation. At the same time, the introduction of the risk function enables the material-energy conversion model to reflect the output of equipment under risk.

C. THE RISK FLUID MOSAIC MODEL OF OMIES

Fluid Mosaic Model (FMM) is a hypothetical model of membrane structure in biology. The model describes that the cell membrane structure is formed by inlaying a movable globular protein in a lipid bilayer. During the transmission process, Globulin is an important carrier for the transmembrane transport of substances. In OMIES, the device is like a cell lipid bilayer, which forms the basic skeleton of the system. The material flow and energy flow are like globular proteins, which are embedded in the basic skeleton to carry the input and output of the system. Therefore, the structure of OMIES can be equivalent to biological membrane FMM. In addition, the energy-material flow analysis starts from the energy flow model, the material flow model, and the energy-material flow feedback model, and analyzes the material-energy transfer and transformation process in OMIES [24]. Risk can be further expressed by the system's material-energy transfer and transformation, so OMIES energy flow and material flow are considered as risk carriers. The structure of OMIES is similar to FMM. The energy flow and material flow in the structure are considered as risk carriers. Therefore, based on the introduction of risk factors and the establishment of a risk matrix, a risk fluid mosaic model (RFMM) is proposed to describe the system risk flow process, as shown in Figure 3. However, due to the differences in the operation mode and structure of each part in the system, RFMM cannot generalize all risks, and needs to be modeled separately for each part's characteristics.

Therefore, according to the above analysis, establish a distributed model based on RFMM for the following four parts

with different characteristics: Energy to Energy Risk Flow Model (EERFM), material-energy risk Material to Energy Risk Flow Model (MERFM), Material to Material Risk Feedback Model (MMRFM), and Energy to Material Risk Feedback Model (EMRFM). This distributed model is based on the system material-energy flow analysis process, which reflects the flow conditions of risk in the four parts of material flow, energy flow, energy-material flow coupling, and process feedback of OMIES. The distributed modeling approach used in this section based on the system structure risk flow mosaic model applies to both OMIES overall risks and individual parts of OMIES risks, which comprehensively characterizes system risks.

1). Energy-energy risk flow matrix

$$\underbrace{\begin{bmatrix} O_1 \\ O_2 \\ \vdots \\ O_i \end{bmatrix}}_{O} = \underbrace{\begin{bmatrix} \rho_{11} & \rho_{12} & \cdots & \rho_{1i} \\ \rho_{21} & \rho_{22} & \cdots & \rho_{2i} \\ \vdots & \vdots & \ddots & \vdots \\ \rho_{i1} & \rho_{i2} & \cdots & \rho_{ii} \end{bmatrix}}_{\rho} \left(\underbrace{\begin{bmatrix} e_{11} & e_{12} & \cdots & e_{1i} \\ e_{21} & e_{22} & \cdots & e_{2i} \\ \vdots & \vdots & \ddots & \vdots \\ e_{i1} & e_{i2} & \cdots & e_{ii} \end{bmatrix}}_{e} \underbrace{\begin{bmatrix} I_1 \\ I_2 \\ \vdots \\ I_i \end{bmatrix}}_{I} \right) \tag{7}$$

where vector **o** represents the energy output matrix; matrix ρ represents the risk flow matrix; matrix **e** represents the energy conversion relationship matrix; vector **I** represents the energy input matrix.

2). Material-energy risk flow matrix

$$\underbrace{\begin{bmatrix} E_1^1 \\ \vdots \\ E_r^1 \\ H_{r+1}^1 \\ \vdots \\ H_n^1 \end{bmatrix}}_{EN1} = \underbrace{\begin{bmatrix} \delta_{11}^c & \delta_{12}^c & \cdots & \delta_{1n}^c \\ \vdots & \vdots & \ddots & \vdots \\ \delta_{r1}^c & \delta_{r2}^c & \cdots & \delta_{rn}^c \\ \delta_{(r+1)1}^z & \delta_{(r+1)2}^z & \cdots & \delta_{(r+1)n}^z \\ \vdots & \vdots & \ddots & \vdots \\ \delta_{n1}^z & \delta_{n2}^z & \cdots & \delta_{nn}^z \end{bmatrix}}_{\delta} \times \left(\underbrace{\begin{bmatrix} c_{11} & c_{12} & \cdots & c_{1n} \\ \vdots & \vdots & \ddots & \vdots \\ c_{r1} & c_{r2} & \cdots & c_{rn} \\ z_{(r+1)1} & z_{(r+1)2} & \cdots & z_{(r+1)n} \\ \vdots & \vdots & \ddots & \vdots \\ z_{n1} & z_{n2} & \cdots & z_{nn} \end{bmatrix}}_{Eq1} \underbrace{\begin{bmatrix} M_1^1 \\ M_2^1 \\ M_3^1 \\ \vdots \\ M_{n-1}^1 \\ M_n^1 \end{bmatrix}}_{M1} \right) \tag{8}$$

where vector **EN1** represents the energy flow output matrix; δ represents the material-energy risk flow matrix; **Eq1** represents the material-energy conversion relationship matrix; vector **M1** represents the material flow input matrix.

3). Energy-material risk feedback matrix

$$\underbrace{\begin{bmatrix} M_1^2 \\ M_2^2 \\ M_3^2 \\ \vdots \\ M_{m-1}^2 \\ M_m^2 \end{bmatrix}}_{M2} = \underbrace{\begin{bmatrix} \sigma_{11}^l & \sigma_{12}^l & \cdots & \sigma_{1m}^l \\ \vdots & \vdots & \ddots & \vdots \\ \sigma_{k1}^l & \sigma_{k2}^l & \cdots & \sigma_{kn}^l \\ \sigma_{(k+1)1}^s & \delta_{(k+1)2}^s & \cdots & \sigma_{(k+1)n}^s \\ \vdots & \vdots & \ddots & \vdots \\ \sigma_{m1}^s & \sigma_{m2}^s & \cdots & \sigma_{mm}^s \end{bmatrix}}_{\sigma 1} \times \left(\underbrace{\begin{bmatrix} l_{11} & l_{12} & \cdots & l_{1m} \\ \vdots & \vdots & \ddots & \vdots \\ l_{k1} & l_{k2} & \cdots & l_{km} \\ s_{(m+1)1} & s_{(m+1)2} & \cdots & s_{(k+1)m} \\ \vdots & \vdots & \ddots & \vdots \\ s_{m1} & s_{m2} & \cdots & s_{mm} \end{bmatrix}}_{Eq2} \underbrace{\begin{bmatrix} E_1^2 \\ \vdots \\ E_k^2 \\ H_{k+1}^2 \\ \vdots \\ H_m^2 \end{bmatrix}}_{EN2} \right) \tag{9}$$

where vector **M2** represents the material flow output matrix; σ**1** represents the energy-material risk flow matrix; **Eq2** represents the energy-material conversion relationship matrix; vector **EN2** represents the energy flow input matrix.

4). Material-Material Risk Flow Matrix

$$\underbrace{\begin{bmatrix} M_1^3 \\ M_2^3 \\ M_3^3 \\ \vdots \\ M_{m-1}^3 \\ M_m^3 \end{bmatrix}}_{M3} = \underbrace{\begin{bmatrix} \sigma_{11}^l & \sigma_{12}^l & \cdots & \sigma_{1m}^l \\ \vdots & \vdots & \ddots & \vdots \\ \sigma_{k1}^l & \sigma_{k2}^l & \cdots & \sigma_{kn}^l \\ \sigma_{(k+1)1}^s & \delta_{(k+1)2}^s & \cdots & \sigma_{(k+1)n}^s \\ \vdots & \vdots & \ddots & \vdots \\ \sigma_{m1}^s & \sigma_{m2}^s & \cdots & \sigma_{mm}^s \end{bmatrix}}_{\sigma 2} \times \left(\underbrace{\begin{bmatrix} l_{11} & l_{12} & \cdots & l_{1m} \\ \vdots & \vdots & \ddots & \vdots \\ l_{k1} & l_{k2} & \cdots & l_{km} \\ s_{(m+1)1} & s_{(m+1)2} & \cdots & s_{(k+1)m} \\ \vdots & \vdots & \ddots & \vdots \\ s_{m1} & s_{m2} & \cdots & s_{mm} \end{bmatrix}}_{Eq3} \underbrace{\begin{bmatrix} W_1 \\ \vdots \\ W_k \\ W_{k+1} \\ \vdots \\ W_m \end{bmatrix}}_{W} \right) \tag{10}$$

where vector **M3** represents the material flow output matrix; σ**2** represents the energy-material risk flow matrix; **Eq3** represents the material-material conversion relationship matrix; vector **W** represents the material flow input matrix. In formulas (9)-(10), **M2** and **M3** contain both the same substance and different substances, which need to be distinguished according to the corresponding part. Since $\sigma 1$ and σ**2**, **Eq2** and **Eq3** are also in the feedback part, their elements represent the same, but have different values.

Each element in the substance and energy conversion matrix of the above model is the calculated value of the

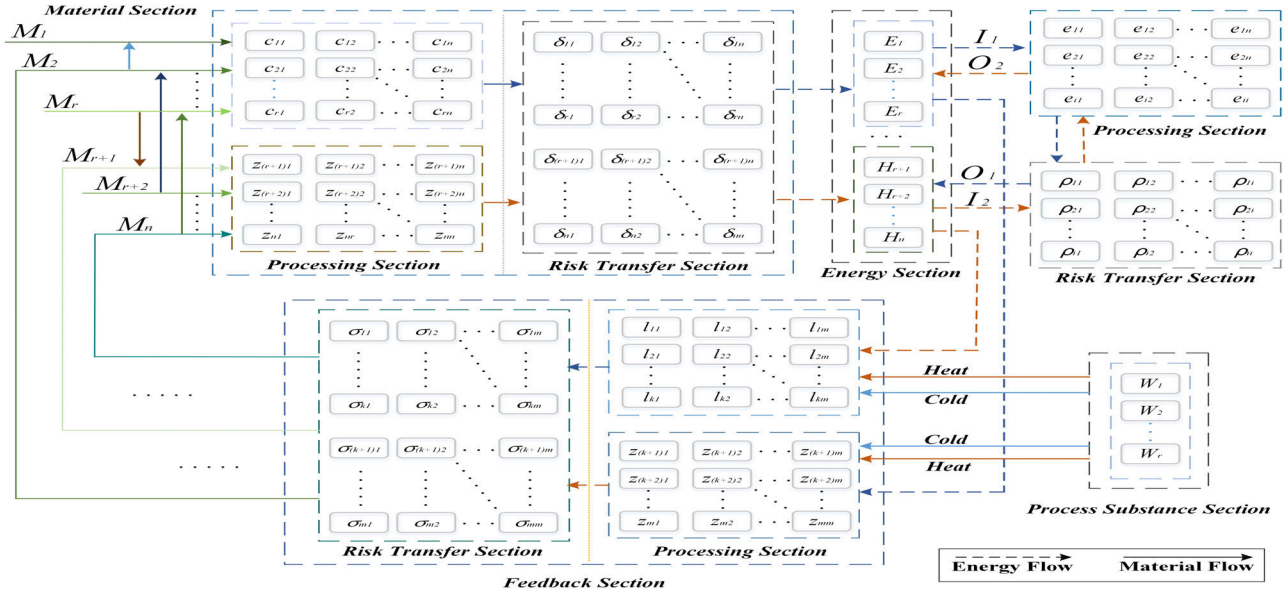

FIGURE 3. Material-energy flow diagram of OMIES.

conversion relationship of the corresponding part [24], and each element of the risk flow matrix is the value of the operating state of the corresponding equipment under risk. The value is between 0 and 2, 0 means no output of the device, 1 means normal output, greater than 1 means overrun of the device, and a value between $0 \sim 1$ means derated operation of the device, the specific value is determined by the operating characteristics of the device.

The model proposed in this article uses energy and material flow as a risk carrier, covering all the transfer and changes of energy and matter in OMIES. It analyzes the OMIES from four aspects: energy-energy, matter-energy, matter-material, and energy-material. The transfer process of random risk with energy and material flow describes the real-time risk status of OMIES in more detail.

III. QUANTITATIVE ANALYSIS AND ASSESSMENT PROCESS OF SYSTEMIC RISK

A. RISK INDICATORS

Based on the risk index of the independent energy supply system [20], the system decoupling and energy network delisting risk indicators shown in Table 1 for the OMIES are proposed to characterize the state of material-energy coupling of the risk to the system and the impact on the structural stability of the energy grid.

B. MULTI-WEIGHTED SYSTEM RISK GRADING

Risk grading is a quantitative analysis of the severity of each risk. Through the risk grading, the system risk status can be analyzed. Risk grading is divided into two parts: one is the grading of the severity of each risk index, and the grading scheme is shown in Appendix A; the second is the grading of the degree of influence of various risk indicators on the overall system. The traditional method for quantifying the overall risk of the system is to multiply the risk probability by the risk consequences, and then grade it according to the obtained results [18]. However, this method cannot directly express the overall system's risk status due to the different dimensions of risk and consequences. Therefore, scientists first grade each risk index and then quantify the severity of the system risk [19], such as equations (11)-(12). This method improves the risk probability and different dimensions. When multiple risks occur simultaneously, this method cannot quantify the overall system risk. Therefore, in this section, a multi-weighted system risk grading model is proposed, such as equations (13)-(15). The model is divided into three types according to the degree of risk, and then the weighted sum of the three types of risk severity, which is the average of various levels, and finally the weighted sum of the obtained result and the severity level of risk probability. The result is the overall risk profile of the system. The model takes into account the different risk dimensions and the situation when multiple risk situations occur, laying a good foundation for the quantitative analysis of OMIES risks.

TABLE 1. OMIES risk indicator.

Grid	Gas Net	Hot Net	Micro Integrated Energy System
Voltage Offset	Insufficient Air Supply	Insufficient Heat Supply	Electric-Gas-Thermal Decoupling
Power Limit			Energy Net Decommissioning
Load Transfer			Outage of Important Users

$$G = round(\varepsilon_0 G_{SP} + \xi_0 G_{CS}) \tag{11}$$

$$\varepsilon_0 + \xi_0 = 1 \tag{12}$$

$$L = round(\varepsilon_1 L_{SP} + \xi_1 \times (\varsigma_1 \frac{\sum_{t1=1}^{N1} L_{t1}^{CS1}}{N1} + \varsigma_2 \frac{\sum_{t2=1}^{N2} L_{t2}^{CS2}}{N2} + \varsigma_3 \frac{\sum_{t3=1}^{N3} L_{t3}^{CS3}}{N3})) \quad (13)$$

$$\varepsilon_1 + \xi_1 = 1 \quad (14)$$

$$\varsigma_1 + \varsigma_2 + \varsigma_3 = 1 \quad (15)$$

where G and L represent the overall risk level of the system; G_{SP} and L_{SP} represent the risk occurrence probability level; G_{CS}, L_{t1}^{CS1}, L_{t2}^{CS2}, L_{t3}^{CS3} are the severity levels of each risk consequence; ε_0, ξ_0, ε_1, ξ_1, ς_1, ς_2, ς_3 indicate corresponding weights; *round*(•)indicates rounding.

C. THE RISK ASSESSMENT PROCESS OF OMIES

Based on the characteristics of OMIES, the following evaluation steps are designed in consideration of the gas grid, heat grid, and grid operation strategies:

Step 1: Enter the original data to form system information;

Step 2: Analyze the system energy flow to form the initial state of the system;

Step 3: Perform status sampling to determine whether there is a faulty device. If not, proceed to step 3, and if so, proceed to step 4.

Step 4: Generate fault information, analyze the network topology, and determine whether there is a decoupling phenomenon. If not, go to step 6;

Step 5: Network reconstruction, analysis and reconstruction of network energy flow;

Step 6: Energy flow analysis to determine whether there are accident consequences, if not, go to step 8, if so, go to step 7;

Step 7: Analysis of risk incidents of the system;

Step 8: Determine whether the sampling is completed, if yes, go to step 9, if no, return to step 3;

Step 9: End.

IV. CASE STUDIES

In order to verify the rationality of the model and evaluation scheme in this paper, taking an offshore oil and gas platform in the Bohai Sea as an example, different scenarios were designed to evaluate the risk of the system. Since the model in this paper is also applicable to the OMIES subsystem, this section considers single and double faults, analyzes the impact of the coupled system on the power system, and evaluates the OMIES risk situation. Because the coupled system has the same analysis method for the gas network and heat network, no analysis is done in this paper.

Scenario 1: Study the risk status of independent grids in OMIES with traditional independent system risk assessments.

Scenario 2: Investigate the risk of power system affected by gas-grid coupling (with diesel supplement).

Scenario 3: Investigate power system risks affected by gas-grid coupling (without diesel).

TABLE 2. Probability of outage of some equipments.

	Gas turbine outage probability	Line outage probability
S1	$2.1032*10^{-4}$	$4.96*10^{-3}$
S2	$8.9968*10^{-4}$	$4.96*10^{-3}$

Scenario 4: Investigate the risk of power system impacted by the coupling of heat networks

Table 2 is a comparison of the outage probability of a gas turbine and a line in different scenarios in scenarios 1 and 2.

S1 is the equipment outage probability of the independent power grid; S2 is the equipment outage probability taking into account the gas-electricity coupling. As shown in Table 2, taking into account the gas network coupling, the probability of gas turbine outage is greater than the probability of outage in the independent power grid, and the line outage probability is the same. It is because the gas turbine is a gas-electric coupling device and will be affected by the coupling system, while the line is an electrical equipment and is not affected by the coupling system. The analysis shows that the traditional outage model does not consider the impact of risk transmission. Although the probability of outage of equipment that takes into account multi-energy coupling is high, it is more helpful to the operation and maintenance of OMIES.

Figure 4 is the risk analysis of a compressor failure (excluding diesel supplement) under RFMM. NC-C indicates the gas supply network connected to the compressor, GT and BT are the gas turbines and steam turbines in this part of the gas supply network, EN4-EN17 and EZ20 are the power nodes and branches that represent risks, and HS is the heat source network, NC-P indicates the associated gas production part of the production process system, the order of the parts indicates the risk order of the system under fault simulation. When a compressor fails, the gas supply of the gas network is reduced by 0.25, which causes greater pressure on the power grid and the heating network. Voltage offsets and power violations occur at the corresponding nodes and branches of the power grid, and the heating network has insufficient heating. And when the gas supply is reduced, the power output of GT and BT is reduced by 0.25 and 0.4, and the grid nodes 4, 5, 11, and 12 have a three-level risk of voltage deviation, while the nodes 14, 15 and 16, 17 have two and one-level voltages, respectively. The above simulation results show the material-to-energy conversion of the equipment under risk, reflecting the risk transfer process from the perspective of material and energy changes. It shows that when using RFMM to characterize risk, the energy-material flow is used as the carrier to convey the system risk more clearly.

Figures 5 and 6 show the first-level risk-related situation of the power system node voltage and branch power obtained through simulation of each scenario. Different risks are faced when the system fails due to the different operating methods of each electrical node and branch. It can be seen from

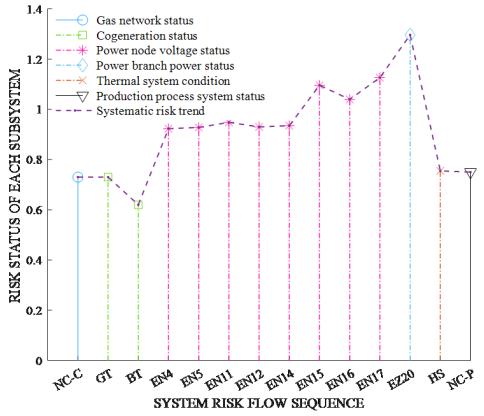

FIGURE 4. OMIES simulation analysis based on RFMM.

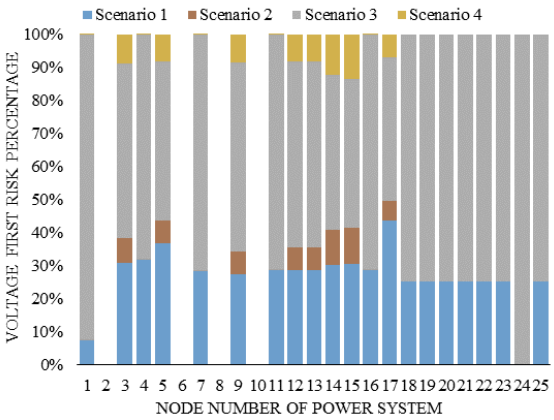

FIGURE 5. Percentage of first risk of power system node voltage in each scenario.

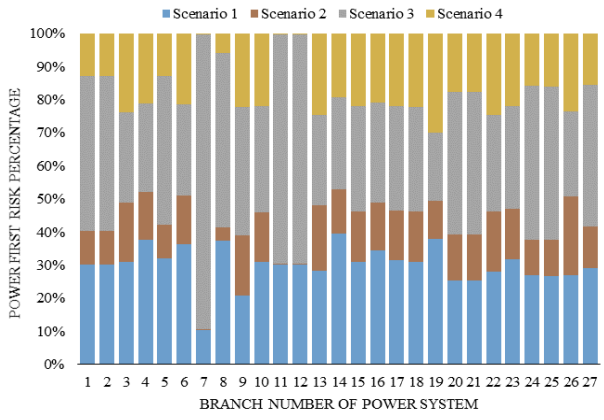

FIGURE 6. Percentage of first risk of branch power in power system in each scenario.

Fig. 5 and Fig. 6 that each node and branch in scenario 3 has the largest proportion of first-level risks, scenario 1 has the second largest proportion of risks, and scenarios 2 and 4 have the smallest proportions. Based on Scenario 1 and the introduction of the gas network in Scenario 2 and Scenario 3 does not affect the operation of all nodes and branches, but because Scenario 2 has diesel as a supplement to the gas supply interruption, there is no need to consider energy

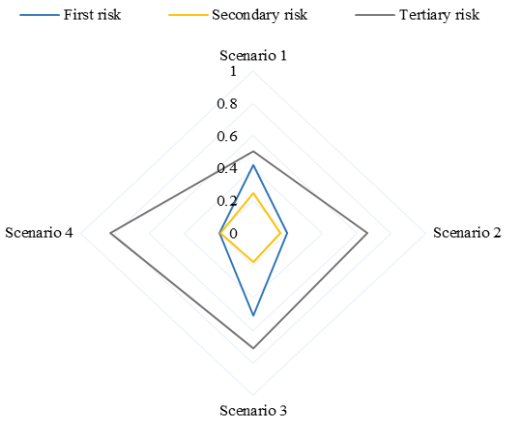

FIGURE 7. Load shearing risk probability graphs of power systems in each scenario.

supply failure caused by gas supply failure Can reduce the risk, so the risk probability of scenario 2 is lower than that of scenario 1. Scenario 3 lacks diesel supplementation, so the uncertainty of system energy supply cannot be ignored. The decrease in gas supply caused by gas network failure will supplement gas and heat by increasing the electrical load, resulting in an increased probability of power system failure. The failure of the heating network affects the production process, causing part of the load to be derated or cut off. Instead, the risk probability of the power node voltage and branch power is reduced, so scenario 4 has the lowest risk ratio. At the same time, Figures 5 and 6 show the probability of first-level risk for each electrical node and branch in the same scenario. Taking scenario 1 in Figure 5 as an example, the probability of the first-level risk for nodes 5, 17 is higher, and node 1 is relatively low. The data is important for the operation and maintenance of the system. The above analysis reflects that it is difficult to reflect the actual risks of OMIES by only performing a risk assessment of an independent system. The risk analysis method based on material-energy flow analysis combines the coupling characteristics of the system to objectively evaluate the risks of OMIES.

Stable load operation is extremely important for offshore platforms. Figure 7 shows the load shedding risk situation in scenarios 1-4. Due to the different fault locations and components of the power grid, the load is divided into two levels, so the load shedding risks are different in each scenario, and the probability of the third level and the first level is higher than the second level. The uncertainty of gas supply in scenario 2 is transformed into system economic risk, so the probability of the first and second load shedding risks is lower than in scenario 1, but because the gas supply interruption of the living platform requires power supplement, the probability of small load removal becomes higher. In scenario 3, the risk of interruption of energy supply is increased, so that the probability of the first- and third-level risks of load shedding will increase. Scenario 4 considers the impact of the heating network and analyzes the load shedding risks at various levels

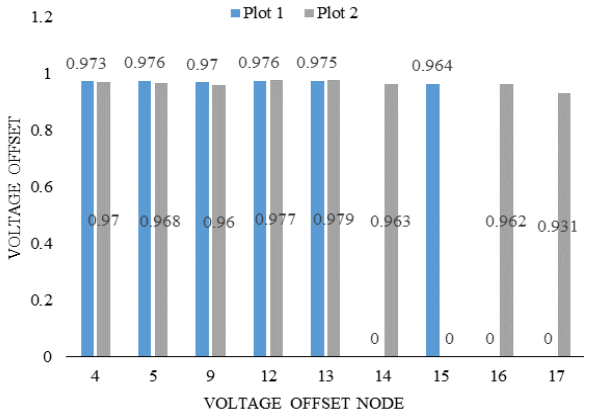

FIGURE 8. Risk of power nodes under preset faults.

TABLE 3. Equipment risk probability under preset faults.

Risk accident	Risk state probability	Risk probability level
Line 9 failure	1.68×10^{-3}	First level
Failure of line 8 and compressor 1	3.649×10^{-7}	Third level

of the power grid. The fault in this article only considers the double, therefore, the probability of primary and secondary risks is low and the probability of tertiary risks is high. The above analysis is mainly based on the impact of gas and heat networks on the power grid. Since the analysis methods of the effects of gas and heat networks on heat networks and power grids and heat networks on gas networks are the same, no further analysis is performed.

In order to evaluate the risk of the system when electricity, gas, and heat work together, this article selects some faults as the source of the risk, and verifies the scientificity of the proposed scheme. With line 9 as the primary failure object (plot 1), line 8 and compressor 1 as the double failure object (plot 2), the system risk was evaluated. Figure 8 shows the risk situation of grid node voltage under a preset fault.

Table 3 is a quantitative description of the probability and level of the preset fault wind, and Table 4 shows the risk situation in this type of scenario. According to the actual operating conditions of OMIES, ε_1 is 0.4, ξ_1 is 0.6, ς_1, ς_2 and ς_3 are 0.6, 0.3, and 0.1 respectively. L_{t1}^{CS1} includes risks for heating network and grid risks, and L_{t2}^{CS2} for gas network risks, L_{t3}^{CS3} is the economic risk, the risk conditions and the overall risk status are shown in the following table:

Table 3 and Table 4 reflect the system risk situation. Taking scenario 1 as an example, when the power connection line 9 is out of service, a power shortage occurs at the nodes with 10 nodes as the source of power, resulting in low voltage quality at some nodes. To ensure system stability, consider Load transfer to maintain the balance of source and load, so there will be transfer risks, which will further lead to gas network risks, energy network decommissioning risks and

TABLE 4. Consequences of system risks under preset faults.

Risk category	Plot 1 Consequences		Plot 2 Consequences	
Load Transfer	2.6%	Tertiary risk		
Insufficient Air Supply	12.3%	Tertiary risk	18.5%	Secondary risk
Energy Net Decommissioning	2	Secondary risk	2	Secondary risk
Economic Losses	3.6	Secondary risk	7.7	Secondary risk
Comprehensive risk level	Secondary risk		Secondary risk	

economic risks. On the other hand, the above simulations show that traditional models are difficult to quantitatively describe the overall system risk when there are multiple risk consequences, but the multi-weighted system risk grading model presented in this paper can quantitatively describe the overall system risk situation.

V. CONCLUSIONS

This paper constructs a risk output model based on risk impact factors for offshore platform output equipment using a unified modeling method. This model improves the problem of traditional output equipment modeling complex and difficult to reflect the relevance of the system structure, and describes the device material-energy conversion relationship of equipment at risk. At the same time, a risk fluid mosaic model is established, which uses energy-material flow as a carrier to describe the risk transfer process from the perspective of material and energy flow. In addition, the risk index of the micro integrated energy system is designed, and a multi-weight system risk grading model is established to quantitatively characterize the system risk. The rationality of the proposed model and method is verified by designing different simulation scenarios for an offshore platform in the Bohai Sea. The simulation results show that in the risk assessment of a single energy system, the risk of OMIES cannot be accurately described because the risk of the occurrence of the risk is relatively low and the effect of the coupled system is ignored. The model proposed in this article takes into account the coupling effects and presents a higher probability of risk. It describes the risk transfer process based on the flow of matter and energy, describes the risk situation, and shows the same system when considering the effects of different coupling systems through the comparison of different scenarios risk form. At the same time, the model in this paper improves the current situation that traditional risk grading models cannot reflect multiple risks. In addition, the simulation results show that the traditional single energy system risk assessment method cannot adapt to the development status of the multi-energy coupling system. The OMIES risk assessment needs to start from the material-energy coupling

TABLE 5. Probability grading scheme for each risk system.

Risk level	Risk state occurrence probability
Tertiary risk	1×10^{-8}—1×10^{-4}
Secondary risk	1×10^{-4}—1×10^{-3}
First risk	$>1\times10^{-3}$

TABLE 6. Risk consequence ranking scheme.

Risk category	Tertiary risk	Secondary risk	First risk
Voltage Offset	0.02~0.05	0.05~0.1	>0.1
Power Limit	0.9~1	1~1.2	>1.2
Load Transfer	0.02~0.05	0.05~0.1	>0.1
Insufficient Air Supply	0.1~0.15	0.15~0.3	>0.3
Insufficient Heat Supply	0.015~0.025	0.025~0.035	>0.035
Electric-Gas-Thermal Decoupling	1	2	≥3
Energy Net Decommissioning		2	≥3
Outage of Important Users	I	II	III
Economic losses(yuan)	10000-30000	30000-100000	>100000

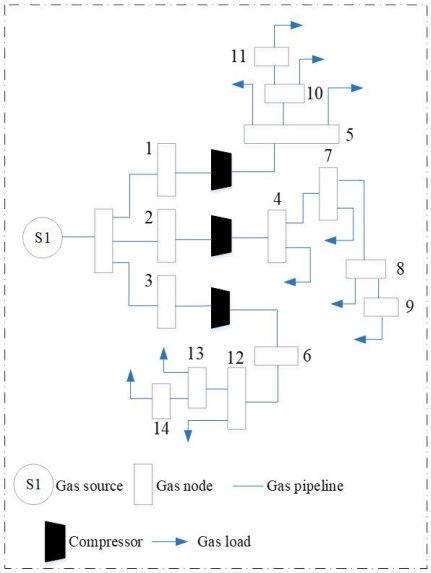

FIGURE 9. Simulation gas network topology.

and take into account the impact of the coupled system to describe the risk more comprehensively.

APPENDIXES

APPENDIX A

Tables 5 and 6 show the ratings of the risk occurrence probability and risk consequence severity of the offshore micro integrated energy system.

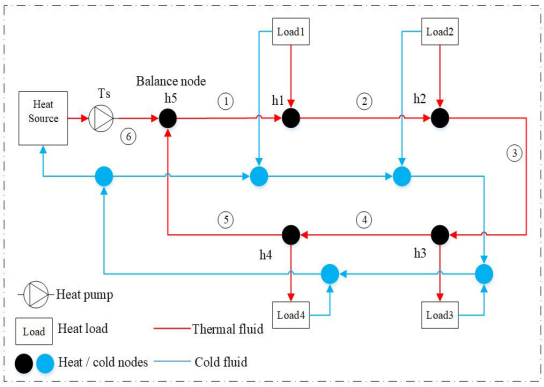

FIGURE 10. Simulation heat network topology.

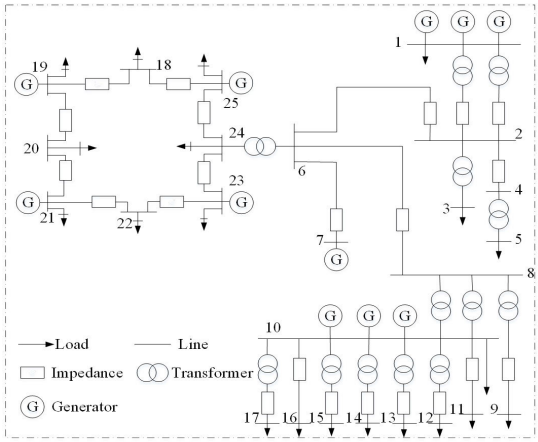

FIGURE 11. Simulation grid topology.

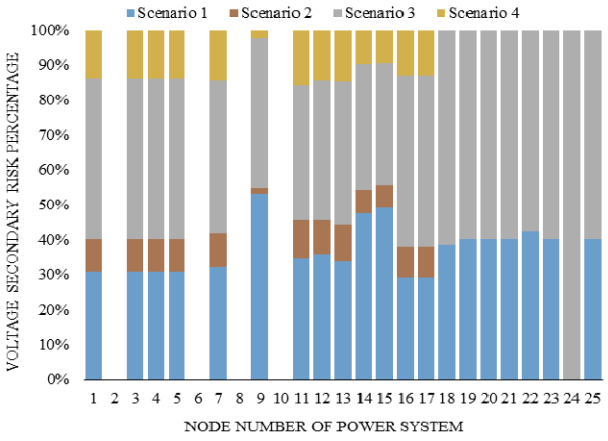

FIGURE 12. Percentage of secondary risk of power system node voltage in each scenario.

APPENDIX B

Figures 9-11 show the gas network, heat network, and power network topology. of the offshore micro-energy system.

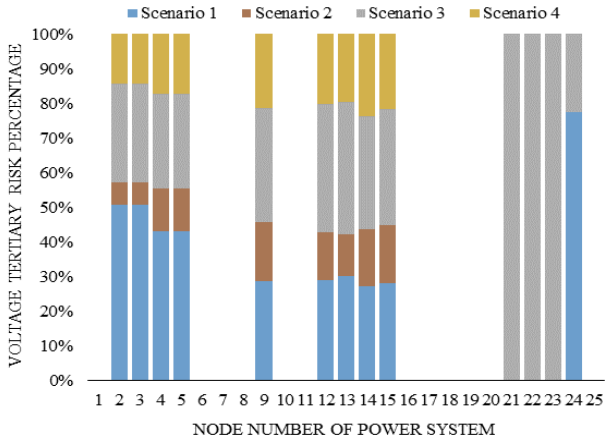

FIGURE 13. Percentage of tertiary risk of power system node voltage in each scenario.

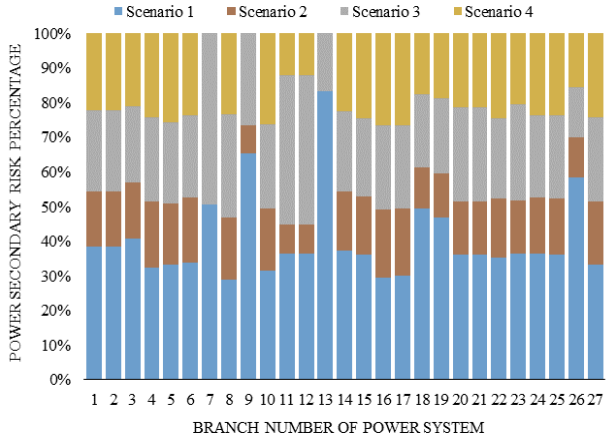

FIGURE 14. Percentage of secondary risk of branch power in power system in each scenario.

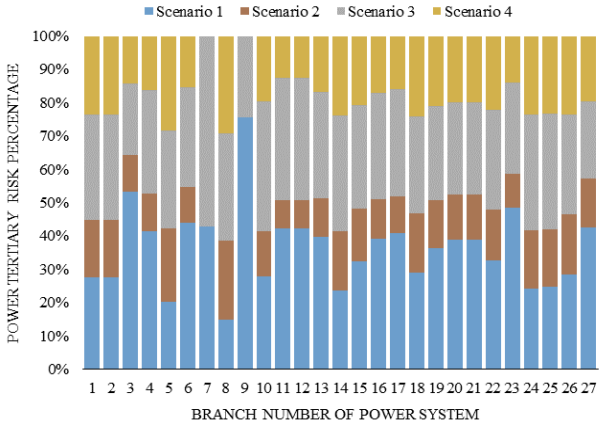

FIGURE 15. Percentage of tertiary risk of branch power in power system in each scenario.

APPENDIX C

The power system node voltage and branch power secondary and tertiary risk results obtained from simulation are shown in Figures 12-15.

REFERENCES

[1] A. Zhang *et al.*, "Fuzzy stochastic programming of offshore mies including electricity and associated gas storage," *Proc. CSEE*, vol. 39, no. 20, pp. 5915–5925 and 6172, 2019.
[2] T.-V. Nguyen and S. de Oliveira, Jr., "System evaluation of offshore platforms with gas liquefaction processes," *Energy*, vol. 144, pp. 594–606, Feb. 2018.
[3] A. Zhang, H. Zhang, M. Qadrdan, X. Li, and Q. Li, "Energy hub based electricity generation system design for an offshore platform considering CO_2-mitigation," *Energy Procedia*, vol. 142, pp. 3597–3602, Dec. 2017.
[4] D. Yi, Y. Jiang, Y. Song, C. Guo, W. Jin, and L. Zhang, "Review of risk assessment for energy Internet part: Physical level," *Proc. CSEE*, vol. 36, no. 14, pp. 3806–3817, 2016.
[5] C. Yan, "Risk assessment studies for new generation energy system," *Power Syst. Technol.*, vol. 43, no. 01, pp. 12–22, 2019.
[6] D. YaXian and M. DaJun, "Operation optimization method of distributed system for combined cooling heating and power," *J. Electr. Power Sci. Technol.*, vol. 32, no. 1, pp. 55–64, 2017.
[7] J. Wang, Z. Yan, M. Wang, S. Ma, and Y. Dai, "Thermodynamic analysis and optimization of an (organic rankine cycle) ORC using low grade heat source," *Energy*, vol. 49, pp. 356–365, Jan. 2013.
[8] J. Yu, L. Guo, M. Ma, S. Kamel, W. Li, and X. Song, "Risk assessment of integrated electrical, natural gas and district heating systems considering solar thermal CHP plants and electric boilers," *Int. J. Electr. Power Energy Syst.*, vol. 103, pp. 277–287, Dec. 2018.
[9] S. Zhang, "Reliability evaluation of electricity-heat integrated energy system with heat pump," *CSEE J. Power Energy Syst.*, vol. 4, no. 4, pp. 425–433, 2018.
[10] H. Wang, X. Wang, Z. Ren, X. Wang, and Z. He, "Risk assessment of integrated energy system based on electrical-thermal energy flow," in *Proc. 2nd IEEE Conf. Energy Internet Energy Syst. Integr. (EI)*, Beijing, China, Oct. 2018, pp. 1–6.
[11] Y. Liu, Y. Su, Y. Xiang, J. Liu, L. Wang, and W. Xu, "Operational reliability assessment for gas-electric integrated distribution feeders," *IEEE Trans. Smart Grid*, vol. 10, no. 1, pp. 1091–1100, Jan. 2019.
[12] H. Yang, Y. Zhang, Y. Ma, D. Zhang, L. Sun, and S. Xia, "Reliability assessment of integrated energy system considering the uncertainty of natural gas pipeline network system," *IET Gener., Transmiss. Distrib.*, vol. 13, no. 22, pp. 5033–5041, Nov. 2019.
[13] Y. Huang and G. Li, "Reliability evaluation of distributed integrated energy systems via Markov chain Monte Carlo," in *Proc. IEEE Conf. Energy Internet Energy Syst. Integr.*, Nov. 2017, pp. 1–5.
[14] M. Bao, Y. Ding, C. Shao, Y. Yang, and P. Wang, "Nodal reliability evaluation of interdependent gas and power systems considering cascading effects," *IEEE Trans. Smart Grid*, early access, Mar. 23, 2020, doi: 10.1109/TSG.2020.2982562.
[15] C. Yan, Y. Hu, Z. Bie, and C. Wang, "MILP-based combined power and natural gas system risk assessment in energy Internet," in *Proc. 2nd IEEE Conf. Energy Internet Energy Syst. Integr. (EI)*, Beijing, China, Oct. 2018, pp. 1–6.
[16] G. Li, Y. Kou, J. Jiang, Y. Lin, and Z. Bie, "Researches on the reliability evaluation of integrated energy system based on energy hub," in *Proc. China Int. Conf. Electr. Distrib. (CICED)*, Xi'an, China, Aug. 2016, pp. 1–9.
[17] H. Liu, "Impact evaluation of operation strategies of multiple energy storage system on reliability of multi-energy microgrid," *Automat. Electr. Power Syst.*, vol. 43, no. 10, pp. 36–45, 2019.
[18] L. Junzhe, S. Lu, Z. Quansheng, and L. Jingjing, "Research on evaluation system of operation risk assessment and application in henan power gird," in *Proc. IEEE PES Asia–Pacific Power Energy Eng. Conf. (APPEEC)*, Hong Kong, Dec. 2014, pp. 1–5.
[19] Y. Wang, "Construction and application of power grid operation risk assessment and rating system," *Automat. Electr. Power Syst.*, vol. 39, no. 8, pp. 141–148, 2015.
[20] Y. Cao, W. Wang, Z. Lu, and H. Li, "The operating risk evaluation of power system with a large scale of wind farms considering uncertainty of wind power prediction and extreme weather," in *Proc. 2nd IET Renew. Power Gener. Conf. (RPG)*, Beijing, China, 2013, pp. 1–4.
[21] Y. Sun, L. Cheng, H. Liu, and S. He, "Power system operational reliability evaluation based on real-time operating state," in *Proc. Int. Power Eng. Conf.*, Singapore, vol. 2, 2005, pp. 722–727.
[22] J. He, L. Cheng, and Y. Sun, "Analysis of Components' reliability modeling based on real-time operating conditions," in *Proc. Int. Conf. Power Syst. Technol.*, Chongqing, China, Oct. 2006, pp. 1–5.

[23] L. Cheng, H. Liu, X. Zou, and Y. Sun, "Short-term reliability online evaluation basing on transient state probability," in *Proc. IEEE Power Eng. Soc. Gen. Meeting*, Tampa, FL, USA, Jun. 2007, pp. 1–7.
[24] A. Zhang, H. Zhang, M. Qadrdan, W. Yang, X. Jin, and J. Wu, "Optimal planning of integrated energy systems for offshore oil extraction and processing platforms," *Energies*, vol. 12, no. 4, p. 756, 2019.

ANAN ZHANG (Senior Member, IEEE) received the B.Sc., M.Sc., and Ph.D. degrees in electrical engineering from Sichuan University, China. He is currently a Professor with Southwest Petroleum University. He has published more than 50 articles in refereed journals. His main research interests include offshore power systems, renewable energy generation and its integration, and smart grid applications.

GAOQIANG PENG received the B.S. degree in electrical engineering from the Chengdu Institute of Technology, Chengdu, China, in 2018. He is currently pursuing the M.S. degree in control engineering with Southwest Petroleum University. His research interests include risk assessment of power and integrated energy systems.

WEI YANG (Member, IEEE) received the B.S. and Ph.D. degrees from Sichuan University, China, in 2012 and 2018, respectively. He is currently a Lecturer with the School of Electrical and Information, Southwest Petroleum University, China. His current research interests include plug-in electric vehicle integration, active distribution network planning, and optimal operation.

GUANGLONG QU (Member, IEEE) received the B.S. and Ph.D. degrees from Sichuan University, China. He is currently a Lecturer with the School of Electrical and Information, Southwest Petroleum University, China. His current research interest includes research on power quality analysis and control.

HUANG HUANG received the B.S. degree in electrical engineering from Southwest Petroleum University, Chengdu, China, in 2017, where he is currently pursuing the M.S. degree in control engineering. His research interests include static equivalent and power system control.